Analysis of the High Frequency Series Impedance of GaAs Schottky Diodes by a Finite Difference Technique

Udayan V. Bhapkar, *Student Member, IEEE,* and Thomas W. Crowe, *Senior Member, IEEE*

Abstract—**This paper describes a method to investigate the high frequency series impedance of GaAs Schottky barrier diodes. The analysis uses the finite difference technique to calculate the electromagnetic field within the diode chip based on a solution of Maxwell's equations, and includes high-frequency effects, such as the skin effect, charge carrier inertia, and dielectric relaxation. These effects are shown to greatly increase the series impedance at high frequencies. The finite difference technique is accurate for diode structures that incorporate an epitaxial layer of different doping than the substrate and a non-ideal ohmic contact on the bottom of the chip. An important feature of this analysis is an impedance calculation based on power considerations, rather than the electrostatic potential. The analysis is used to investigate the series impedance as a function of epilayer doping density, anode diameter, chip thickness and ohmic contact resistivity. It is shown that a proposed membrane diode, whose thickness is less than one skin depth, will have a series impedance 30 percent less than that of a comparable standard diode, provided that the ohmic contact has a specific contact resistivity of 10^{-8} Ωcm^2 or less.**

I. Introduction

HETERODYNE receivers have been developed for use at frequencies as high as 3 THz, and have found application in fields such as radio astronomy, plasma diagnostics, and atmospheric chemistry [1]–[3]. These receivers use a non-linear element to mix the radio frequency signal with a local oscillator waveform to convert the signal to a much lower frequency, which can then be amplified and analyzed. GaAs Schottky barrier diodes have proven to be the best mixer elements for use at frequencies in the terahertz range, and improvement of these devices will increase receiver sensitivity and extend the range of the electromagnetic spectrum that can be observed.

A diagram of a GaAs Schottky diode with the ohmic contact on the back surface of the chip is given in Fig. 1, and a scanning electron micrograph of a whisker-contacted chip is shown in Fig. 2. The chip is typically a square of side 100 μm or more, and has thickness of about 125 μm. However, thinner devices, known as membrane diodes, are being investigated [4]. A few thousand anodes of diameter ranging from 0.5 μm to a few microns, are fabricated on the lower doped GaAs epitaxial layer by plating platinum and gold through holes which are photolithographically defined in the oxide layer.

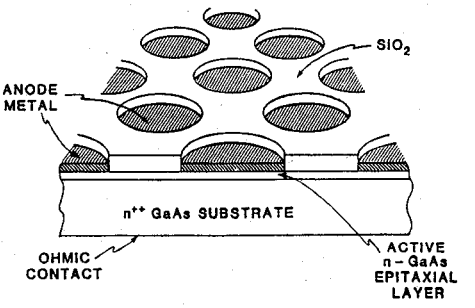

Fig. 1. Schottky diode chip.

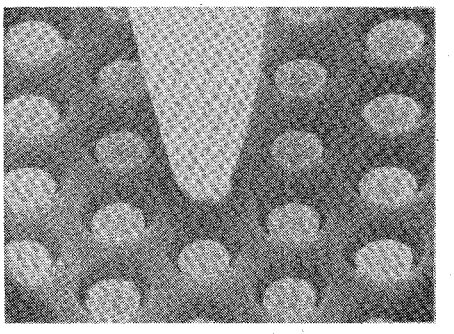

Fig. 2. Scanning electron micrograph of Schottky diode chip with 2 μm diameter anode with whisker contact.

An important consideration in the optimization of Schottky barrier diodes for frequencies greater than 600 GHz is the figure-of-merit cutoff frequency [5], which is proportional to the reciprocal of the product of the series resistance and the junction capacitance. The junction capacitance of a Schottky diode is easily approximated, but the calculation of its high frequency series impedance is complicated by the skin effect, which constricts the current to within a few microns of the outer boundary of the chip for frequencies greater than a few hundred gigahetrtz. To consider this phenomenon, it is necessary to determine the electromagnetic field in the device, a task that is complicated by the awkward boundary conditions of the chip.

Manuscript received July 18, 1991; revised December 30, 1991. This work was supported by the National Science Foundation under grant ECS-8720850.

The authors are with the Semiconductor Device Laboratory, Department of Electrical Engineering, University of Virginia, Charlottesville, VA 22903.

IEEE Log Number 9107026.

Several authors have developed methods to approximate the series impedance of Schottky diodes; however, each of these methods contains one or more serious deficiencies. The first rigorous mathematical analysis of the spreading impedance of a Schottky diode was presented by Dickens [6]. Champlin and Eisenstein have shown [7] that electron inertia and dielectric effects become significant at terahertz frequencies and therefore a complete model of the series impedance must consider these factors. Roos and Wang have extended Dickens' analysis and obtained a series approximation of the substrate spreading resistance that considers these effects, and is highly accurate at frequencies up to the terahertz range [8]. All of the above analyses assume a simplified diode structure with uniform conductivity in the semiconductor material and an ideal ohmic contact surrounding the diode chip. However, most state-of-the-art terahertz diodes incorporate epitaxial layers of lower doping than the heavily doped substrate, and have ohmic contacts on the bottom of the chip. Accurate, analytic solutions cannot be readily obtained for these more complicated configurations. Campbell and Wrixon have performed a finite element analysis of the resistance of Schottky barrier diode chips with epitaxial layers [9] and with ohmic contacts in various locations of the chip. However, their technique uses the *electrostatic* field equations, which are strictly valid only at zero frequency, and the simplistic approximation that the current density is uniform within one skin depth of the chip surface and zero further within the chip. Although their analysis possesses the capability to model various unusual anode shapes, it does not consider the *electromagnetic* field at high frequencies. Another important phenomenon in Schottky diodes that has not been addressed is that a potential function cannot be uniquely defined at high frequencies. This may not be a significant problem for frequencies below about 100 GHz, but represents a major failing of the prior analyses at terahertz frequencies, when the dimensions of the device are much greater than both the wavelength and the skin depth.

Recently, Seidel and Crowe [4] have proposed a finite difference technique that can be used to overcome the many limitations of the previous analyses. They used a simple program to demonstrate that the electromagnetic fields in the chip could be accurately calculated, provided that cylindrical symmetry is assumed. We have also used the finite difference method, and have incorporated effects such as charge carrier inertia and dielectric relaxation, and have added the capability to consider epitaxial layers. In addition, our calculation of the series impedance does not rely on the concept of potential. The resulting analysis is the first that considers all of the following aspects:

1) An epitaxial layer of doping density different from that in the substrate.
2) A non-ideal (resistive) ohmic contact on the bottom of the chip.
3) The skin effect through solution of Maxwell's curl equations.
4) Charge carrier inertia.
5) Dielectric relaxation.
6) An impedance calculation based on power rather than potential.

The finite difference program (FDP) is discussed in Section II of this paper. The difference equation, the boundary conditions, the model of the semiconductor conductivity and the ohmic contact are presented. In Section III the results of the program are discussed. Specifically, we have studied the effect of the anode size, epitaxial layer doping density, chip thickness, and ohmic contact resistance on the series impedance and the current path. A brief summary and conclusion are presented in Section IV.

II. The Finite Difference Program

For the purposes of this study, we assume that a single anode at the center of the chip is contacted by the whisker. To simplify the calculation, we will also assume the chip to be cylindrical, rather than square shaped. These assumptions will not appreciably change the results.

The finite difference program (FDP) solves the electromagnetic field equations on a two dimensional (r, z) lattice that covers the epitaxial, substrate, and ohmic contact regions of the diode chip. After hundreds of iterations, the electromagnetic field relaxes to a final solution. The lattice has a variable density to increase the speed and accuracy of the calculation. The energy density of the electric and magnetic fields are then obtained, and the impedance is calculated as the ratio of the dissipative and reactive power to the square of the total current. The FDP also provides a capability for plotting the current contours within the chip, a useful visual tool.

A. Difference Equation

Dickens has shown that when azimuthal symmetry is imposed, Maxwell's curl equations may be combined to form a single partial differential equation [6]. In cylindrical coordinates, this equation is expressed as

$$\frac{\partial^2 Q}{\partial r^2} - \frac{1}{r}\frac{\partial Q}{\partial r} + \frac{\partial^2 Q}{\partial z^2} - \gamma^2 Q = 0, \tag{1}$$

where Q is defined in terms of the magnetic field as

$$Q = rH_\theta, \tag{2}$$

where γ is the propagation constant in the semiconductor, defined as

$$\gamma = [j\omega\mu_o(\sigma + j\omega\epsilon)]^{1/2} \tag{3}$$

where ω is the angular frequency, σ is the conductivity, ϵ, is the permittivity, and μ is the permeability. The nonvanishing components of the electric field are given by

$$E_r = \frac{j\omega\mu_o}{r\gamma^2}\frac{\partial Q}{\partial z} \tag{4}$$

and

$$E_z = -\frac{j\omega\mu_o}{r\gamma^2}\frac{\partial Q}{\partial r}. \tag{5}$$

Equation (1) cannot be solved analytically for the boundary conditions of actual diodes with the ohmic contact at the bottom of the chip, and is further complicated when a discontinuity in the propagation constant exists, as is the case in diodes with epitaxial layers and non-ideal ohmic contacts. However, the differential equation is readily converted to a difference equation which can be solved for the complicated chip structure under investigation. The basic form of the difference equation, neglecting the variable density grid and the complex form of Q, is given by

$$Q_{\text{new}\,r,z} = \frac{\dfrac{Q_{r+1,z}+Q_{r-1,z}}{\Delta r^2} - \dfrac{Q_{r+1,z}-Q_{r-1,z}}{2r\,\Delta r} + \dfrac{Q_{r,z+1}+Q_{r,z-1}}{\Delta z^2}}{\gamma^2 + \dfrac{2}{\Delta r^2} + \dfrac{2}{\Delta z^2}} \tag{6}$$

where Δr and Δz are the distances between grid points. Provided that the point is not on one of the diode's boundaries, (considered in Section C) this difference equation is used to obtain a new value of $Q_{r,z}$ in terms of its four nearest neighbors $Q_{r-1,z}$, $Q_{r+1,z}$, $Q_{r,z-1}$, and $Q_{r,z+1}$. The mesh on which Q is solved has a size ($r_{\max}$, $z_{\max}$) that depends on the frequency and the dimensions of the diode being simulated.

The equation for Q as it appears in the program is slightly more complicated than (6) because Q is complex and because the grid has an unequal density of lattice points. The unequal density grid is a feature of the program in which the intervals Δr and Δz have different lengths in different regions of the diode chip. The greatest concentration of grid points is near the anode, the region having the highest current density. The regions near the chip boundaries also have a high current density, and therefore the grid points in these regions are also closely spaced. In the regions of the chip that are relatively far from the anode and the boundaries, however, the current density is low and has a small gradient, and therefore the lattice points are spaced farther apart.

We performed numerous FDP simulations using various densities of grid points. The final grid densities used reflected a compromise between accuracy and CPU time. In general, the grid densities were chosen so that halving the lattice spacing produced a change in the overall impedance of no more than a few percent. From these studies, we estimate that the predicted impedance values are precise to within $\pm 5\%$.

B. Electron Inertia and Displacement Current

The propagation constant γ, defined in (2), considers the effect of electron inertia on the conduction current, and also considers the displacement current. A simplified treatment of the electron inertia involves a complex conductivity [10], given by

$$\sigma = \frac{\sigma_o}{1 + j\omega\tau} \tag{7}$$

where σ_o is the (real) dc conductivity and τ is the electron relaxation time. In this analysis, the electron relaxation time is approximated in terms of the macroscopic semiconductor properties as

$$\tau = \frac{m^*\mu}{q} \tag{8}$$

where m^* is the electron effective mass, q is the electronic charge, and μ is the semiconductor mobility. The mean electron relaxation time in highly doped GaAs corresponds to a frequency around 1 THz, which suggests that effects due to electron inertia may become significant around this frequency. The form of (7) indicates that an inductive component of the current density arises from the nonzero electron mass. While this model of the electron inertia does not consider the diverse scattering mechanisms individually, it has been shown to provide a useful and reasonably accurate model of the bulk semiconductor impedance at high frequencies [10].

The electron inertia and the displacement current contribute imaginary terms of opposite sign to the propagation constant. At a frequency known as the plasma frequency [10], given by

$$\omega_p = \left(\frac{\sigma_o}{\tau\epsilon}\right)^{1/2}, \tag{9}$$

the electron inertia and the displacement current form a resonance. The plasma frequency depends on the doping level of the semiconductor, which affects both the electron mobility and the conductivity. According to the above equations, the plasma frequency is about 3 THz and 20 THz in n-GaAs doped at 1×10^{17} cm^{-3} and 5×10^{18} cm^{-3}, respectively. However, the plasma resonance has a rather large half-width, and can therefore be a significant effect even at a few terahertz. The FDP considers plasma resonance effects by including the complex conductivity and the displacement current in the propagation constant.

C. Boundary Conditions

A solution of the difference equation requires the imposition of boundary conditions at the edges of the chip and at discontinuities in the semiconductor material. We divide the chip into distinct regions, as shown in Fig. 3. Each region has its own boundary condition, and therefore requires a different algorithm to compute Q.

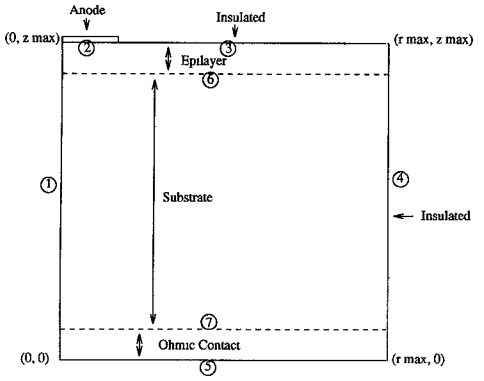

Fig. 3. Regions of the FDP lattice.

The boundary condition in Region 1 follows from (3) and the requirement that H_θ be finite on the diode's central axis. This leads to

$$Q = 0 \quad \text{for} \quad r = 0. \tag{10}$$

The second boundary condition requires the normal component of the electric field to be zero on the boundary between the semiconductor and the insulated regions, represented as Regions 3 and 4. Using (4) and (5) we obtain the boundary conditions for these surfaces. In Region 3, the top surface of the chip, we have

$$\frac{\Delta Q}{\Delta r} = 0. \tag{11}$$

Thus Q is constant along the upper surface. Similarly, in Region 4, the outer wall of the chip, we have

$$\frac{\Delta Q}{\Delta r} = 0, \tag{12}$$

which requires Q to be constant along this surface as well. The magnitude of this constant determines the amount of current flowing through the diode. Since the constant is arbitrary, for simplicity we choose

$$Q = 1 \quad \text{for} \quad r = r_{\max}$$

and

$$Q = 1 \quad \text{for} \quad z = z_{\max} \quad \text{and} \quad r > a, \tag{13}$$

where a is the anode radius. It can be shown that with this condition, the total current through the diode is 2π A [11].

The boundary conditions in Regions 2 and 5, the anode and the ohmic contact, respectively, are not exactly modeled in the finite difference algorithm. It can be shown that at nonzero frequency, the tangential component of the electric field at the anode is not zero, and therefore the anode is not precisely an equipotential [6]. Fortunately, at frequencies up to several terahertz, the tangential component of the electric field is much smaller than the normal component, and therefore using the equipotential approximation introduces only a small error [6], [11]. We therefore impose the following boundary condition at the anode and the ohmic contact:

$$\frac{\Delta Q}{\Delta z} = 0. \tag{14}$$

It should be noted that the diode mount (beneath the ohmic contact) and the whisker present additional impedance contributions that depend on their geometry. These impedances may contain significant inductive components. In addition, the magnetic field surrounding the diode itself will also add a small inductive component. However, these inductances can be controlled by the circuit designer, and are not modeled by the FDP.

The interfaces between the epilayer and the substrate (Region 6), and between the substrate and the ohmic contact (Region 7), require a form of the difference equation that takes into account the variation in the propagation constant γ on either side of the interface. This difference equation is given by

$$Q_{\text{new}\,r,z} = \frac{\dfrac{\gamma_z^2(Q_{r+1,z} + Q_{r-1,z})}{\Delta r^2} - \dfrac{\gamma_z^2(Q_{r+1,z} - Q_{r-1,z})}{2r\,\Delta r} + \dfrac{\gamma_{z-1}^2 Q_{r,z+1} + \gamma_z^2 Q_{r,z-1}}{\Delta z^2}}{\gamma_z^2\gamma_{z-1}^2 + \dfrac{2\gamma_z^2}{\Delta r^2} + \dfrac{2(\gamma_z^2 + \gamma_{z-1}^2)}{\Delta z^2}}, \tag{15}$$

where γ_z and γ_{z-1} are the propagation constants in the regions above and below the coordinate (r, z), respectively.

D. Ohmic Contact Model

State-of-the-art, high-frequency Schottky barrier diodes have alloyed ohmic contacts on the bottom surface of the chip [4], [12]. A rigorous analysis of the electromagnetic field in this portion of the chip would require knowledge of the variation in the conductivity and propagation constant throughout the alloy region. This is beyond the scope of the present work. As a simplification we have approximated the ohmic contact as a thin layer of material, of thickness t_{oc}, and conductivity σ_{oc}, such that the resistance per unit area of the layer is equal to the specific resistivity of the ohmic contact R_{sc}. These quantities are related through the equation

$$\sigma_{oc} = \frac{t_{oc}}{R_{sc}}. \tag{16}$$

We have found that the choice of t_{oc} is not critical in determining the series impedance of the chip, but does affect the convergence time of the calculation. Therefore, values of t_{oc} that lead to the fastest convergence have been used. Since we assume a purely resistive ohmic contact, the conductivity in the ohmic contact region is real at all frequencies and the propagation constant is readily obtained from this conductivity.

It is important to note that our model of the ohmic con-

tact is highly simplified. However, in spite of its simplicity, the model is sufficient to obtain the impedance and the current distribution of a Schottky diode, and is a vast improvement compared to previous analyses which assumed an ideal ohmic contact with zero resistance.

E. Program Iteration

When the iteration commences, all Q values are set to zero, except along the insulated boundaries (Regions 3 and 4), where Q is set to unity. The Q values are then calculated for each lattice point using the algorithms described above, and the process is repeated until the Q array approaches a limiting configuration.

In order to reduce the convergence time, a process known as over-relaxation is used, in which the difference between the new and old values of Q is multiplied by a constant, w, known as the over-relaxation factor [13]. In the over-relaxation technique, the new value of Q is replaced by

$$Q_{\text{new}} \leftarrow Q_{\text{old}} + w(Q_{\text{new}} - Q_{\text{old}}) \tag{17}$$

where w is greater than or equal to one. We have generally used w ranging from 1.5 to 1.75 in our simulations.

F. Impedance Calculation

One of Maxwell's equations,

$$\nabla \times \boldsymbol{E} = -j\omega\mu\boldsymbol{H}, \tag{18}$$

states that the electric field $\boldsymbol{E}$ is not curl-free at nonzero frequency. This means that at nonzero frequency, the line integral of the electric field is in general dependent on the choice of path. Thus, it is not possible to uniquely define a potential function, except at dc. At fairly low frequencies, using the electrostatic approximation (that is, curl-free electric fields) may not present a major source of error, and many workers have used this approach. However, at frequencies above a few hundred gigahertz, the complete Maxwell equations must be used to obtain accurate solutions of the electromagnetic field. The electric fields obtained from these solutions are not curl-free, and it follows that a potential function cannot be unambiguously defined. At high frequencies, therefore, we must resort to a slightly more complicated calculation of the impedance.

The integral of the Poynting vector over a closed surface enclosing the chip, indicated by P,

$$P = -\oint_S \boldsymbol{E} \times \boldsymbol{H}^* \cdot d\boldsymbol{S}, \tag{19}$$

represents the rate of energy flow into the chip, where $d\boldsymbol{S}$ is the normal differential element to the surface. The real part of this integral represents the power dissipated in the chip, and the imaginary part represents the stored energy. The impedance is calculated according to the formula

$$Z_s = \frac{P}{I \cdot I^*} \tag{20}$$

where I is the total current flowing through the chip, which with our choice of boundary conditions is equal to 2π. According to the divergence theorem, (19) can be written as

$$P = -\int_V \nabla \cdot (\boldsymbol{E} \times \boldsymbol{H}^*)\, dV \tag{21}$$

where dV is the differential volume element. Using vector identities, it is easy to show that P may be expressed as [14]

$$P = -\int_V j\omega\mu_o \boldsymbol{H} \cdot \boldsymbol{H}^*\, dV - \int_V (\sigma + j\omega\epsilon)^* \boldsymbol{E} \cdot \boldsymbol{E}^*\, dV \tag{22}$$

where σ is the complex conductivity. Using (7), (20), and (22), the impedance may be expressed as

$$R_s = \text{Re}\,(Z_s) = \frac{1}{4\pi^2} \int_V \frac{\sigma_o}{1 + (\omega\tau)^2} \boldsymbol{E} \cdot \boldsymbol{E}^*\, dV \tag{23}$$

$$X_s = \text{Im}\,(Z_s) = \frac{\omega}{4\pi^2} \int_V \left[\mu_o \boldsymbol{H} \cdot \boldsymbol{H}^* - \epsilon \boldsymbol{E} \cdot \boldsymbol{E}^* + \frac{\tau}{1 + (\omega\tau)^2} \boldsymbol{E} \cdot \boldsymbol{E}^* \right] dV. \tag{24}$$

Notice that the reactance contains three terms. The magnetic field and the displacement current contribute inductive and capacitive terms, respectively, both of which increase with the frequency. The additional inductive term arises from the nonzero momentum relaxation time τ, and is associated with the electric field.

III. Results

A. Current Contours

Figs. 4(a)–(c) show the current contours, as generated by the FDP, in Schottky diodes of various thicknesses at a frequency of 1 THz. The simulations assume a specific contact resistivity of $1 \times 10^{-8}\ \Omega\text{cm}^2$, which is low enough so that the resistance of the ohmic contact is negligible. The diode parameters are tabulated in Table I, and unless indicated otherwise, apply to all of the diodes simulated in this paper. The current contours show ten lines, each of which represents ten percent of the total current traversing the diode. The dashed lines indicate the interfaces between the epilayer and the substrate, and between the substrate and the ohmic contact. Note that the r and z axes are drawn to different scales. The figures shown are representative of three distinct patterns in the current distribution present in diodes. Fig. 4(a) shows the current contours in a diode whose thickness is much greater than one skin depth, δ_s. In such diodes the current, after initially flowing downward through the epitaxial layer, flows radially outward in the substrate, just beneath the epilayer. Over 90 percent of the current exists within about two skin depths of the epilayer. After reaching the cylindrical

TABLE I
DIODE PARAMETERS

anode radius	0.25 μm
chip radius	50.0 μm
t_{epi}	0.046 μm
t_{sub}	5.0 μm
t_{oc}	0.1 μm
N_{sub}	4.5×10^{18} cm^{-3}
N_{epi}	1.0×10^{18} cm^{-3}
R_{sc}	1.0×10^{-8} Ωcm^2

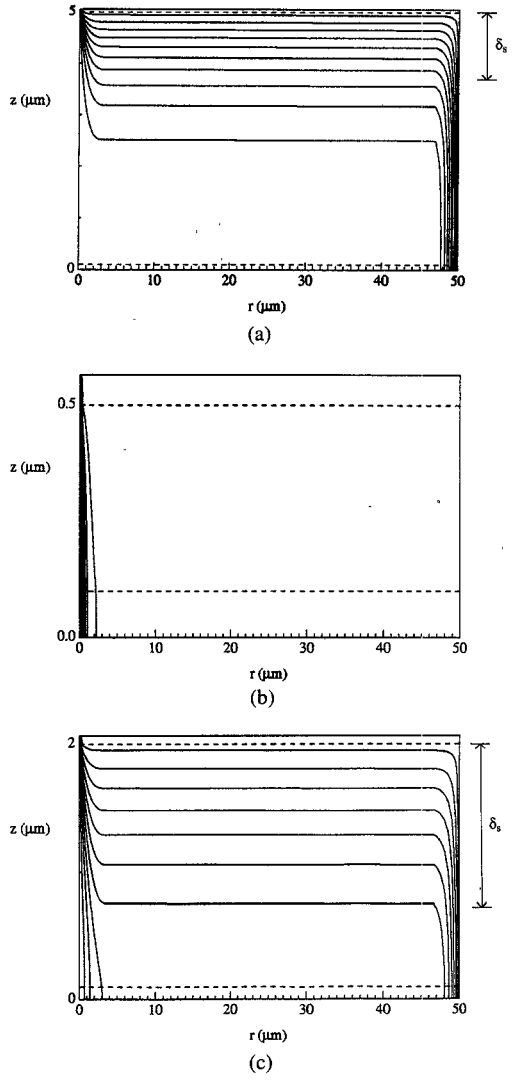

Fig. 4. (a) Current contour, diode with 5 μm substrate at 1 THz. (b) Current contour, diode with 0.5 μm substrate at 1 THz. (c) Current contour, diode with 2 μm substrate at 1 THz.

outer wall, the current flows straight downward, and is again confined to within about two skin depths of the chip boundary. Fig. 4(b) shows the current distribution in a membrane diode whose thickness is much less than one skin depth. Most of the current flows in a vertical path directly from the anode to the ohmic contact at the bottom of the chip, and the regions of the diode chip far from the anode have negligible current density. Fig. 4(c) shows the current distribution in a diode whose substrate thickness is close to one skin depth. Such diodes have characteristics of each of the two cases discussed above. The current splits into two components: the "radial" component, which is dominant in thick diodes, and the "vertical" component, which is dominant in thin membrane diodes. The current distribution in all diodes operated at frequencies greater than several gigahertz follows one of these three patterns.

B. Impedance and Frequency

Fig. 5 shows the total series impedance as a function of frequency.[1] The series resistance increases gradually with frequency; this is due primarily to the decreasing skin depth at higher frequencies. The series inductance, however, increases far more rapidly with frequency than does the series resistance, especially at frequencies greater than about 1 THz. This increase in the inductance is due to both the skin effect, associated with the magnetic field, and the nonzero electron inertia. The series inductance can be minimized by choosing very highly doped material for high frequency devices; however, the diode parameters for the simulations presented here were held constant to specifically show the frequency dependence.

C. Impedance and Chip Thickness

Fig. 6 shows the total series impedance as a function of the chip thickness at a frequency of 1 THz. Both the real and imaginary components of the impedance decrease sharply as the chip thickness is reduced below about one skin depth. In thicker chips, the impedance increases with thickness, at a slow, constant rate. These findings suggest that thin membrane diodes with nearly ideal ohmic contacts may offer significantly less overall series impedance than thick devices.

The calculations indicate that reductions of over 30 percent in the overall diode series resistance can be achived by fabricating diodes that are 0.5 μm thick, compared to typical 125 μm thick diodes. Diodes of 2 μm thickness may offer a reduction in the series resistance of about 10 percent over standard diodes. It should be emphasized that these improvements assume the use of very low resistance ohmic contacts having a specific contact resistivity of 1×10^{-8} Ωcm^2, a standard not usually achieved with most contact technologies.

D. Impedance and Anode Radius

Fig. 7 shows the overall series impedance as a function of the anode radius for a diode 2 μm in thickness. The other diode parameters are the same as previously given. For the range of anode radii shown, the impedance is roughly proportional to the reciprocal of the anode radius.

In addition to the series resistance, a crucial factor in device performance is the $R_s C_{jo}$ product, which is related to the reciprocal of the cut-off frequency. We have cal-

[1] In each graph, symbols indicate results of FDP simulations; the lines are linear interpolations between these values.

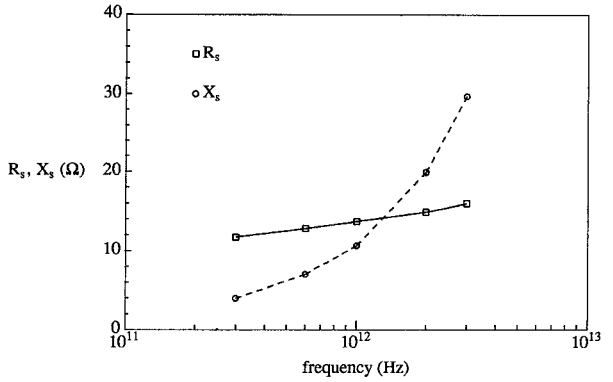

Fig. 5. Series impedance versus frequency.

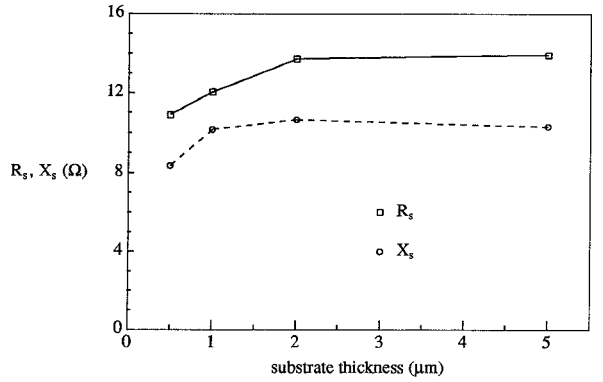

Fig. 6. Series impedance versus substrate thickness at 1 THz.

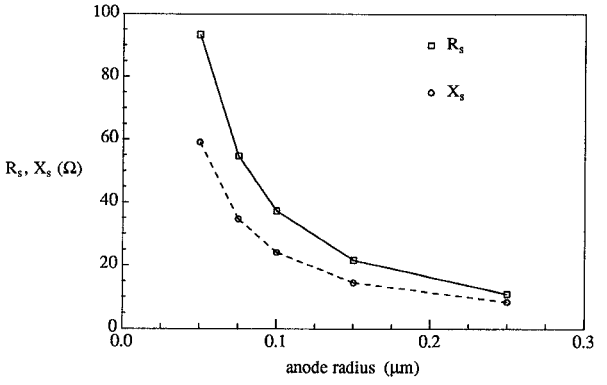

Fig. 7. Series impedance versus anode radius at 1 THz.

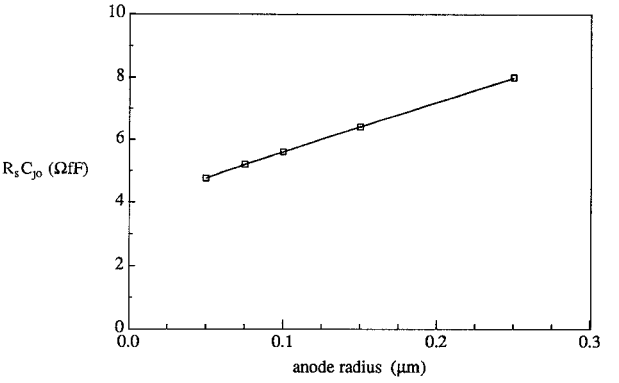

Fig. 8. $R_s C_{jo}$ versus anode radius at 1 THz.

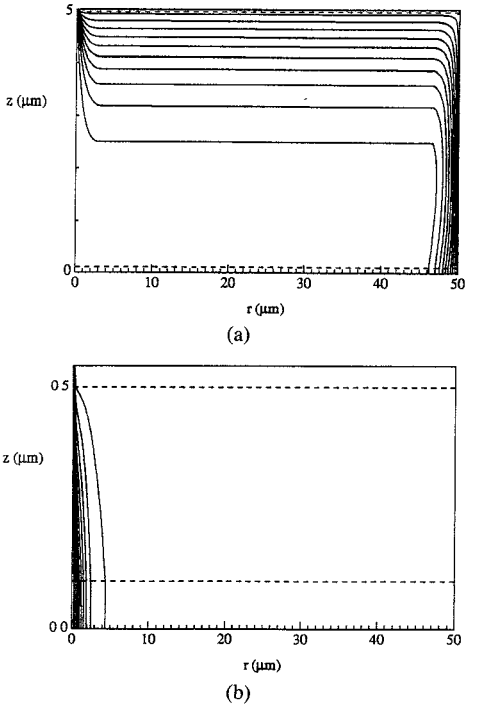

Fig. 9. (a) Current contour, diode with 5 μm substrate and $R_{sc} = 10^{-6}$ Ωcm^2 at 1 THz. (b) Current contour, diode with 0.5 μm substrate and $R_{sc} = 10^{-6}$ Ωcm^2 at 1 THz.

culated the zero-biased junction capacitance C_{jo} from [15]

$$C_{jo} = \frac{\epsilon A}{W} + \frac{3\epsilon A}{2a}, \tag{25}$$

where A is the anode area, W is the depletion layer width at zero-bias, given by

$$W = \left(\frac{2\epsilon V_{bi}}{qN_{epi}}\right)^{1/2}, \tag{26}$$

N_{epi} is the epilayer doping concentration, and V_{bi} is the barrier height in the semiconductor, which is assumed to be equal to 1.0 V in GaAs. The second term in (25) is due to the effects of fringing of the electric field around the anode edges. Fig. 8 shows that $R_s C_{jo}$ increases monotonically with the anode radius. These results suggest that improvements in technology to permit the fabrication of anodes as small as 0.1 μm in radius will yield substantial increases in the cut-off frequency of Schottky diodes.

E. Non-Ideal Ohmic Contacts

To study the effect of non-ideal ohmic contacts on series impedance, we obtained impedances and curent contours from FDP simulations of diodes with specific contact resistivities in the range from 10^{-7} to 10^{-5} Ωcm^2. The contour plots, shown in Fig. 9(a) and (b), show that the current spreads slightly near the high resistance ohmic contact at the bottom of the substrate. The series impedance as a function of chip thickness is shown in Fig. 10 for various specific contact resistances. The graph indicates that in devices of thickness less than about 2 μm, the value of the specific contact resistivity has a significant effect on the overall series resistance, whereas in

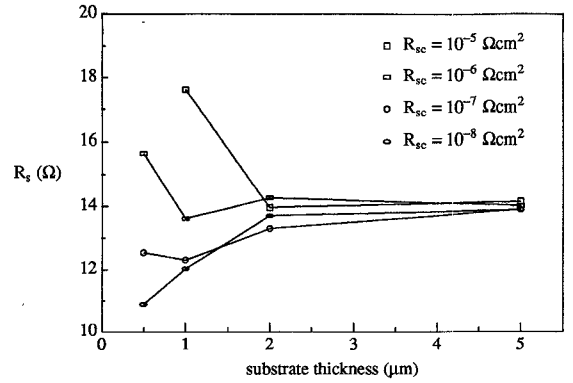

Fig. 10. Series resistance versus chip thickness for various specific contact resistivities at 1 THz. Please note that the FDP calculations have an error of ±0.5 Ω.

thicker chips, the value of the specific contact resistivity is not critical. Furthermore, diodes with specific contact resistivity of 10^{-8} Ωcm^2, show the greatest decrease in total series resistance as the chip thickness is reduced below one skin depth. By contrast, diodes with specific contact resistivity greater than or equal to 10^{-6} Ωcm^2 obtain their minimum series resistance when their thickness is around one skin depth. These findings suggest that to obtain the lowest possible series resistance, it is crucial to develop very thin membrane diodes with very low resistivity ohmic contacts. If ohmic contacts with specific contact resistivity greater than about 10^{-7} Ωcm^2 are used, the potential advantage of membrane diodes over standard diodes is not nearly as great.

IV. Conclusion

In this paper we have presented a finite difference calculation of the series impedance of Schottky barrier diodes. This is the first such analysis that obtains a solution to the complete Maxwell's equations and obtains the impedance based on power considerations, while also being able to consider diodes with moderately doped epitaxial layers and non-ideal ohmic contacts on the bottom of the chip. Furthermore, the use of the complete Maxwell equations in the analysis automatically incorporates the skin effect, the displacement current, and the electron inertia, which should not be neglected at terahertz frequencies.

The calculations show that at terahertz frequencies, there is a gradual increase in the series resistance, and a much sharper rise in the series inductance. This is due to both the skin effect and the electron inertia. We demonstrate that the proposed membrane diode will substantially reduce the series impedance by making the current path much shorter than in diodes of greater thickness. We also show that the full potential of the membrane diode will be realized only if it is fabricated with ohmic contacts having a specific contact resistivity of 10^{-8} Ωcm^2 or less. Diodes slightly thicker than one skin depth may be fabricated with higher resistance ohmic contacts, and still offer reductions in the series impedance compared to that of standard diodes, although the improvement will not be as great as in the previous case.

This algorithm is being used in the design and analysis of diodes for use at frequencies up to several terahertz. A method to calculate the series impedance of planar diodes, using an algorithm similar to that described in this paper, has also been developed [16]. Diodes with epitaxial materials other than GaAs, such as InGaAs, are also being investigated. The new diodes developed from guidelines presented in this analysis will increase both the sensitivity and maximum operating frequency of submillimeter wave heterodyne receivers.

Acknowledgment

We would like to thank Drs. B. Gelmont and M. Shur of the University of Virginia and Dr. A. Kerr of the National Radio Astronomy Observatory for their reading of the manuscript and many suggestions.

References

[1] H. P. Röser, R. Wattenbach, E. J. Durwen, and G. V. Schultz, "A high resolution spectrometer for 100 μm to 1000 μm and detection of CO (J = 7-6), CO (J = 6-5) and ^{13}CO (J = 3-2)," *Astron. Astrophys.*, vol. 165, 287–299, 1986.

[2] R. Behn, D. Dicken, J. Hackmann, S. A. Salito, M. R. Siegrist, P. A. Krug, I. Kjelberg, B. Duval, B. Joye, and A. Pochelon, "Ion temperature measurement of Tokamak plasmas by collective Thomson scattering of D2O laser radiation," *Phys. Rev. Lett.*, vol. 62, no. 24, pp. 2833–2836, June 1989.

[3] J. W. Waters, "Microwave limb-sounding of the earth's upper atmosphere," *Atmospheric Research*, vol. 23, pp. 391–410, 1989.

[4] L. K. Seidel and T. W. Crowe, "Fabrication and analysis of GaAs Schottky barrier diodes fabricated on thin membranes for terahertz applications," *Int. J. Infrared and Millimeter Waves*, vol. 10, no. 7, July 1989.

[5] T. W. Crowe and R. J. Mattauch, "Analysis and optimization of millimeter and submillimeter wavelength mixer diodes," *IEEE Trans. Microwave Theory Tech.*, vol. MTT-35, no. 2, pp. 159–168, Feb. 1987.

[6] L. E. Dickens, "Spreading resistance as a function of frequency," *IEEE Trans. Microwave Theory Tech.*, vol. MTT-15, no. 2, pp. 101–109, Feb. 1967.

[7] K. S. Champlin and G. Eisenstein, "Cutoff frequency of submillimeter Schottky-barrier diodes," *IEEE Trans. Microwave Theory Tech.*, vol. MTT-26, no. 1, pp. 31–34, Jan. 1978.

[8] O. V. Roos and K. L. Wang, "Conversion losses in GaAs Schottky barrier diodes," *IEEE Trans. Microwave Theory Tech.*, vol. MTT-34, no. 1, pp. 183–186, Jan. 1986.

[9] J. S. Campbell and G. T. Wrixon, "Finite element analysis of skin effect resistance in submillimeter wave Schottky barrier diodes," *IEEE Trans. Microwave Theory Tech.*, vol. MTT-30, no. 5, pp. 744–749, May 1982.

[10] K. S. Champlin, D. E. Armstrong, and P. D. Gunderson, "Charge carrier inertia in semiconductors," *Proc. IEEE*, vol. 52, pp. 677–685, June 1964.

[11] U. V. Bhapkar, "An investigation of the series impedance of GaAs Schottky barrier diodes," M.S. Thesis, University of Virginia, pp. 99–101, May 1990.

[12] W. C. B. Peatman and T. W. Crowe, "Design and fabrication of 0.5 micron GaAs Schottky barrier diodes for low-noise terahertz receiver applications," *Int. J. Infrared and Millimeter Waves*, vol. 11, no. 3, pp. 355–365, 1990.

[13] S. E. Koonin, *Computational Physics*. Menlo Park: Commings Publishing, 1986, p. 143.

[14] J. D. Jackson, *Classical Electrodynamics*, 2nd ed. New York: Wiley, 1975, p. 242.

[15] J. A. Copeland, "Diode edge effects of doping-profile measurements," *IEEE Trans. Electron Devices*, vol. ED-17, no. 4, pp. 404–407, May 1979.

[16] U. V. Bhapkar, T. A. Brennan, and R. J. Mattauch, "InGaAs Schottky barrier diodes for minimum conversion loss and low LO power requirements at terahertz frequencies," in *Proc. Second Int. Symp. on Space Terahertz Techology*, Feb. 26–28, 1991, pp. 371–388.

Udayan V. Bhapkar (S'91) was born in Nagpur, India, on June 10, 1962. He obtained the B.S. degree in physics from the Massachussetts Institute of Technology in 1985, the M.S. degree in physics from the University of Illinois in 1987, and the M.S. degree in electrical engineering from the University of Virginia in 1990, where he is currently working towards the Ph.D. Degree.

He has been a Research Assistant at the University of Virginia since 1988, where his interests have included the numerical modeling and high frequency analysis of Schottky barrier diodes and heterojunctions.

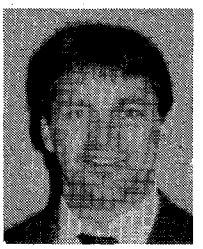

Thomas W. Crowe (S'84–M'87–SM'91) received the B.S. degree in physics from Montclair State College, Montclair, NJ, in 1980. Since that time he has been at the University of Virginia. He received the M.S.E.E. degree from U.Va. in 1982, and the Ph.D. degree in electrical engineering in January 1986.

He became a Research Assistant Professor of Electrical Engineering in March of 1986 and a Research Associate Professor in July of 1991. Since January of 1989 he has been the Director of the Semiconductor Device Laboratory. His main areas of interest are the development of high frequency semiconductor devices and the optimization of solid-state devices for use in low noise submillimeter wavelength receivers. His present research is focussed on the investigation of novel device structures and the use of planar device technologies to allow the routine implementation of heterodyne receivers on space platforms. He also has interests in semiconductor noise theory and the numerical modeling of semiconductor devices.

Dr. Crowe is a member of Sigma Xi, Eta Kappa Nu, and URSI.